

# **Chapter 4**

## **Inertial Navigation System**

An inertial navigation system is an autonomous system that provides information about position, velocity and attitude based on the measurements by inertial sensors and applying the dead reckoning (DR) principle. DR is the determination of the vehicle's current position from knowledge of its previous position and the sensors measuring accelerations and angular rotations. Given specified initial conditions, one integration of acceleration provides velocity and a second integration gives position. Angular rates are processed to give the attitude of the moving platform in terms of pitch, roll and yaw, and also to transform navigation parameters from the body frame to the local-level frame.

### **4.1 Principle of Inertial Navigation**

The principle of inertial navigation is based upon Newton's first law of motion, which states

A body continues in its state of rest, or uniform motion in a straight line, unless it is compelled to change that state by forces impressed on it.

Put simply, this law says that a body at rest tends to remain at rest and a body in motion tends to remain in motion unless acted upon by an outside force. The full meaning of this is not easily visualized in the Earth's reference frame. For it to apply, the body must be in an inertial reference frame (a non-rotating frame in which there are no inherent forces such as gravity).

Newton's second law of motion shares importance with his first law in the inertial navigation system, and states

Acceleration is proportional to the resultant force and is in the same direction as this force.

This can be expressed mathematically as

$$F = ma \quad (4.1)$$

where

$F$  is the force

$m$  is the mass of the body

$a$  is the acceleration of the body due to the applied force  $F$ .

The physical quantity pertinent to an inertial navigation system is acceleration, because both velocity  $v$  and displacement  $s$  can be derived from acceleration by the process of integration. Conversely, velocity and acceleration can be estimated by differentiation from displacement, written mathematically

$$v = \frac{ds}{dt}; a = \frac{dv}{dt} = \frac{d^2s}{dt^2} \quad (4.2)$$

Differentiation is the process of determining how one physical quantity varies with respect to another. Integration, the inverse of differentiation, is the process of summing all rate-of-change that occurs within the limits being investigated, which can be written mathematically as

$$v = \int adt; s = \int vdt = \int \int adtdt \quad (4.3)$$

An inertial navigation system is an integrating system consisting of a detector and an integrator. It detects acceleration, integrates this to derive the velocity and then integrates that to derive the displacement. By measuring the acceleration of a vehicle in an inertial frame of reference and then transforming it to the navigation frame and integrating with respect to time, it is possible to obtain velocity, attitude and position differences. Measurement of the vehicle's rotation is needed for the transformation from the inertial to the navigation frame and for the computation of the attitude of the vehicle.

## 4.2 Physical Implementation of an INS

There are two implementation approaches to an INS: (1) a stable platform system also known as a gimbaled system, and (2) a strapdown system. The components of these systems are shown in Fig. 4.1. In the stable platform, the inertial sensors are mounted on a set of gimbals such that the platform always remains aligned with the navigation frame. This is done by having a set of torque motors rotate the platform in response to rotations sensed by the gyroscopes. Thus the output of the accelerometers is directly integrated for velocity and position in the navigation frame. Since gimbaled systems are mechanically complex and expensive, their use is limited.

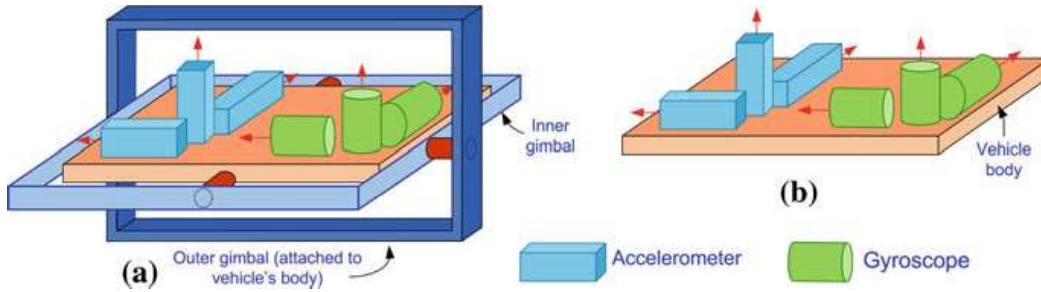


**Fig. 4.1** Arrangement of the components of a gimbaled IMU (*left*) and a strapdown IMU (*right*)

**Table 4.1** Comparison of gimbaled platform and strapdown navigation systems

Characteristics	Strapdown systems	Gimbaled systems
Size	Relatively small	Bigger
Weight	Relatively lighter	Heavy
Performance	High accuracy	Superior performance
Robustness	Highly reliable, immune to shocks and vibrations	High reliability, low immunity to shocks and vibrations

Advances in electronics gave rise to strapdown systems. In these, the inertial sensors are rigidly mounted onto the body of the moving platform and the gimbals are replaced by a computer that simulates the rotation of the platform by software frame transformation. Rotation rates measured by the gyroscopes are applied to continuously update the transformation between the body and navigation frames. The accelerometer measurements are then passed through this transformation to obtain the acceleration in the navigation frame. Strapdown systems are favored for their reliability, flexibility, low power usage, being lightweight and less expensive than stable platforms. The transition to strapdown systems was facilitated by the introduction of optical gyros to replace rotor gyros, and by the rapid development of the processor technology required to perform the computations. Table 4.1 gives a comparison of the major characteristics of the two systems.

An INS can be thought of as consisting of three principal modules: an inertial measurement unit (IMU), a pre-processing unit, and a mechanization module. An IMU uses three mutually orthogonal accelerometers and three mutually orthogonal gyroscopes. The signals are pre-processed by some form of filtering to eliminate disturbances prior to the mechanization algorithm which converts the signals into positional and attitude information. The three major modules of an INS are shown in Fig. 4.2.

### 4.3 Inertial Measurement Unit

The measurements of the acceleration and the rotation of the vehicle are made by a suite of inertial sensors mounted in a unit called the inertial measurement unit (IMU). This holds two orthogonal sensor triads, one with three accelerometers and

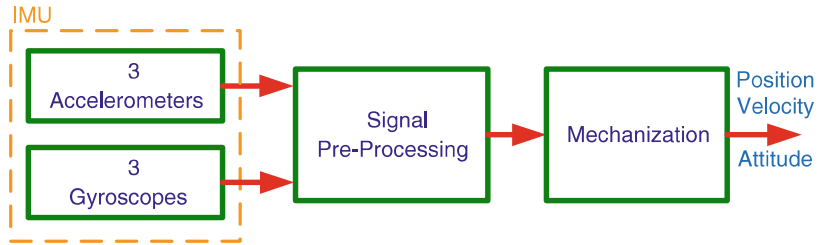


**Fig. 4.2** The principal modules of an inertial navigation system

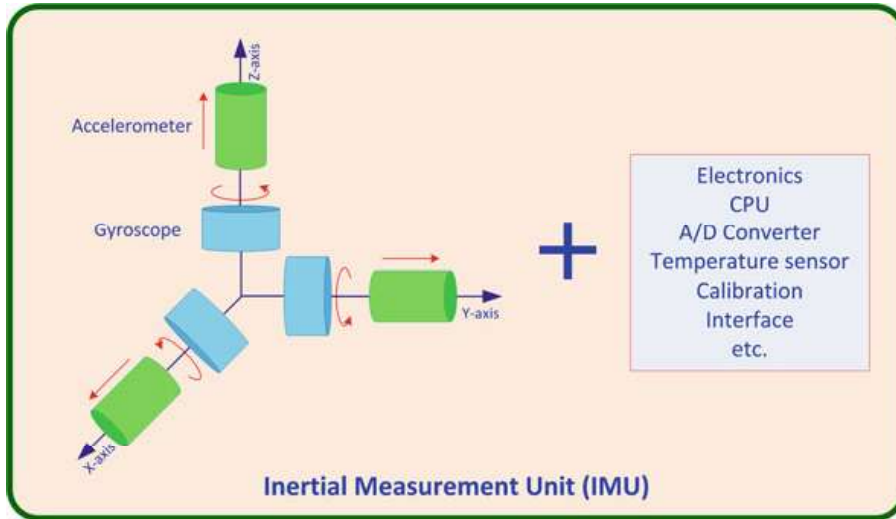


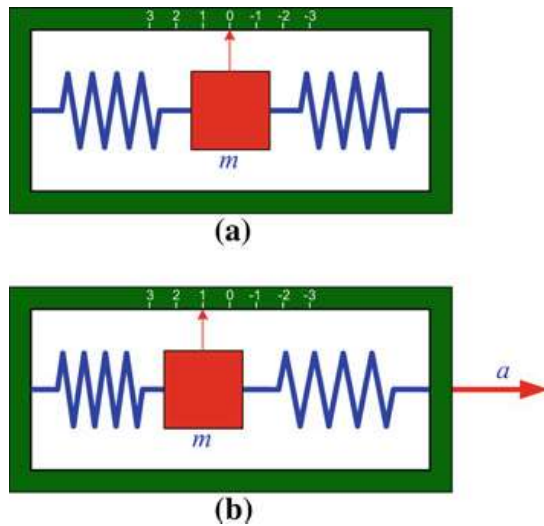
**Fig. 4.3** The components of a typical inertial measurement unit (*IMU*)

the other with three gyroscopes. Accelerometers measure linear motion in three mutually orthogonal directions, whereas gyroscopes measure angular motion in three mutually orthogonal directions. Nominally, the axes of these two triads are parallel, sharing the origin of the accelerometer triad. The sensor axes are fixed in the body of the IMU, and are therefore called the body axes or body frame. Apart from the inertial sensors, the IMU also contains related electronics to perform self-calibration, to sample the inertial sensor readings and then to convert them into the appropriate form for the navigation equipment and algorithms. Figure 4.3 shows the components of a typical IMU.

## 4.4 Inertial Sensors

A brief description of the two main kinds of inertial sensors, accelerometers and gyroscopes, now follows.

**Fig. 4.4** **a** An accelerometer in the null position with no force acting on it, **b** the same accelerometer measuring a linear acceleration of the vehicle in the positive direction (*to the right*)



#### 4.4.1 Accelerometers

An accelerometer consists of a proof mass,  $m$ , connected to a case by a pair of springs as shown in Fig. 4.4. In this case the sensitive axis of the accelerometer is along the spring in the horizontal axis. Acceleration will displace the proof mass from its equilibrium position, with the amount of displacement proportional to the acceleration. The displacement from the equilibrium position is sensed by a pick-off and is then scaled to provide an indication of acceleration along this axis. The equilibrium position is calibrated for zero acceleration. Acceleration to the right will cause the proof mass to move left in relation to the case and (as shown by the scale) indicates positive acceleration.

If the accelerometer is stood on a bench with its sensitive axis vertical in the presence of a gravitational field, the proof mass will be displaced downward with respect to the case, indicating positive acceleration. The fact that the gravitational acceleration is downward, in the *same direction* as the displacement as shown in Fig. 4.5, is sometimes a cause of confusion for the beginners in navigation.

The explanation for this lies in the equivalence principle, according to which, in the terrestrial environment it is not possible to separate inertia and navigation by the accelerometer measurement in a single point. Therefore, the output of an accelerometer due to a gravitational field is the negative of the field acceleration. The output of an accelerometer is called the specific force, and is given by

$$f = a - g \quad (4.4)$$

where

- $f$  is the specific force
- $a$  is the acceleration with respect to the inertial frame
- $g$  is the gravitational acceleration which is  $+9.8 \text{ m/s}^2$ .

**Fig. 4.5** An accelerometer resting on a bench with gravitational acceleration acting on it

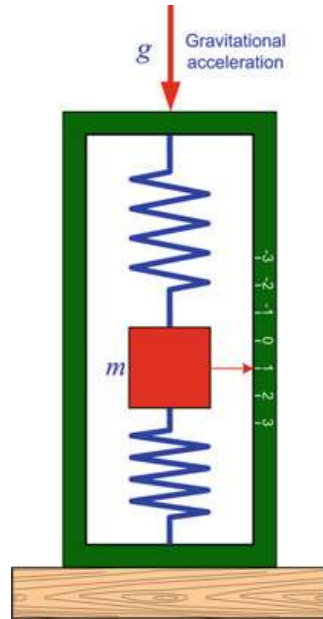
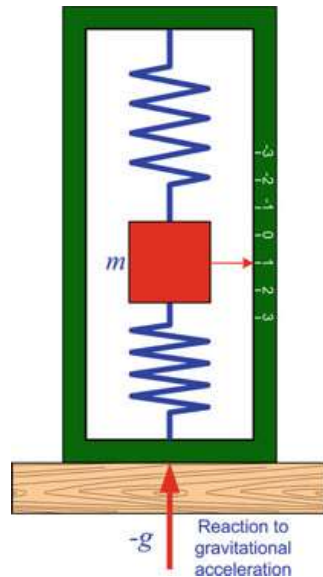


**Fig. 4.6** An accelerometer resting on a bench where reaction to the gravitational acceleration is acting on it



It is this which causes confusion. The easy way to remember this relation is to think of one of two cases. If the accelerometer is sitting on a bench it is at rest so acceleration  $a$  is zero. The force on the accelerometer is the force of reaction of the bench against the case, which is the negative of  $g$  along the positive (upward) direction and therefore causes the mass to move downward (Fig. 4.6).

Or imagine dropping the accelerometer in a vacuum. In this case the specific force read by the accelerometer  $f$  is zero and the actual acceleration is  $a = g$ . To navigate with respect to the inertial frame we need  $a$ , therefore in the navigation equations we convert the output of an accelerometer from  $f$  to  $a$  by adding  $g$ .

#### 4.4.1.1 Accelerometer Measurements

An accelerometer measures translational acceleration (less the gravity component) along its sensitive axis typically by sensing the motion of a proof mass relative to the case. From Eq. (4.4) the output of an accelerometer triad is

$$\mathbf{f} = \mathbf{a} - \mathbf{g} \quad (4.5)$$

where  $\mathbf{f}$  is the specific force vector,  $\mathbf{a}$  is the acceleration vector of the body, and  $\mathbf{g}$  is the gravitational vector. The acceleration  $\mathbf{a}$  can be expressed as the double derivative of the position vector  $\mathbf{r}$ , as

$$\mathbf{a} = \frac{d^2\mathbf{r}}{dt^2} \Big|_i = \ddot{\mathbf{r}} \quad (4.6)$$

The gravitational field vector was earlier shown to be related to the gravity vector as

$$\bar{\mathbf{g}} = \mathbf{g} + \Omega_{ie}\Omega_{ie}\mathbf{r} \quad (4.7)$$

where  $\Omega_{ie}$  is the skew-symmetric matrix representing the rotation of the Earth in the inertial frame.

Substituting Eqs. (4.6) and (4.7) into Eq. (4.5) provides

$$\mathbf{f} = \frac{d^2\mathbf{r}}{dt^2} \Big|_i - \mathbf{g} - \Omega_{ie}\Omega_{ie}\mathbf{r} \quad (4.8)$$

#### 4.4.2 Gyroscopes

To fully describe the motion of a body in 3-D space, rotational motion as well as translational motion must be measured. Sensors which measure angular rates with respect to an inertial frame of reference are called gyroscopes. If the angular rates are mathematically integrated this will provide the change in angle with respect to an initial reference angle. Traditionally, these rotational measurements are made using the angular momentum of a spinning rotor. The gyroscopes either output angular rate or attitude depending upon whether they are of the rate sensing or rate integrating type. It is customary to use the word *gyro* as a short form of the word *gyroscope*, so in the ensuing treatment these words are used interchangeably.

##### 4.4.2.1 Gyroscope Measurements

Gyros measure the angular rate of a body with respect to the navigation frame, the rotation of the navigation frame with respect to the Earth-fixed frame (as it traces

the curvature of the Earth), and the rotation of the Earth as it spins on its axis with respect to inertial space. These quantities are all expressed in the body frame and can be given as

$$\omega_{ib}^b = \omega_{ie}^b + \omega_{en}^b + \omega_{nb}^b \quad (4.9)$$

where

- $\omega_{ib}^b$  is the rotation rate of the body with respect to the i-frame
- $\omega_{nb}^b$  is the rotation rate of the body with respect to the navigation frame (also referred to as the n-frame)
- $\omega_{en}^b$  is the rotation rate of the navigation frame with respect to the e-frame
- $\omega_{ie}^b$  is the rotation rate of the Earth with respect to the i-frame.

Traditional gyroscopes were mechanical and based on angular momentum, but more recent ones are based on either the Coriolis effect on a vibrating mass or the Sagnac interference effect. There are three main types of gyroscope (Lawrence 1998): mechanical gyroscopes, optical gyroscopes, and micro-electro-mechanical system (MEMS) gyroscopes.

## 4.5 Basics of Inertial Navigation

As mentioned before, inertial positioning is based on the simple principle that differences in position can be determined by a double integration of acceleration, sensed as a function of time in a well-defined and stable coordinate frame. Mathematically, we can express this as

$$\Delta P(t) = P(t) - P(t_0) = \int_{t_0}^t \int_{t_0}^t a(t) dt dt \quad (4.10)$$

where

- $P(t_0)$  is the initial point of the trajectory
- $a(t)$  is the acceleration along the trajectory obtained from inertial sensor measurements in the coordinate frame prescribed by  $P(t)$ .

Next, we shall consider examples of navigation in one and two dimensions. An overview of three-dimensional navigation will be given as a preview of the more detailed treatment provided in later chapters.

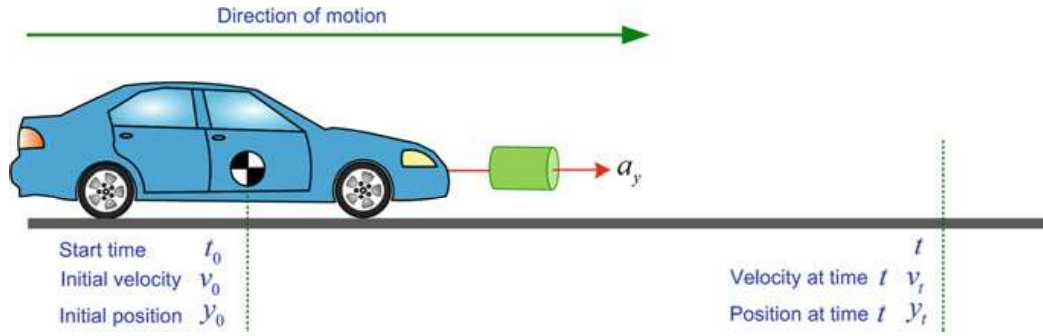


**Fig. 4.7** One-dimensional (1D) inertial navigation, with the green cylinder depicting the accelerometer

### 4.5.1 Navigation in One Dimension

To comprehend the full scale three-dimensional inertial system it is easier to start with an example of a one-dimensional (1D) inertial system with a single axis. For this, consider a vehicle moving in a straight line (i.e. in a fixed direction) as shown in Fig. 4.7. To calculate its velocity and position, which are the only unknowns in this case, we need only a single accelerometer mounted on the vehicle that has its sensitive axis along the direction of motion.

With prior knowledge of the initial position  $y = y_0$  and initial velocity  $v = v_0$  of the vehicle, we are able to calculate its velocity  $v_t$  at any time  $t$  by integrating the output of the accelerometer  $a_y$  as follows

$$v_t = \int a_y dt = a_y t + v_0 \quad (4.11)$$

A second integration will yield the position  $y_t$  of the vehicle at time  $t$

$$\begin{aligned} y_t &= \int v_t dt \\ y_t &= \int (a_y t + v_0) dt \\ y_t &= \frac{1}{2} a_y t^2 + v_0 t + y_0 \end{aligned} \quad (4.12)$$

### 4.5.2 Navigation in Two Dimensions

Extending the concept of navigation from the simple 1D example to 2D makes the implementation more complex, mainly because we need the acceleration to be in the same frame as the coordinate system. This requires the transformation of the acceleration measured by the accelerometers from the INS frame to a stable Earth-

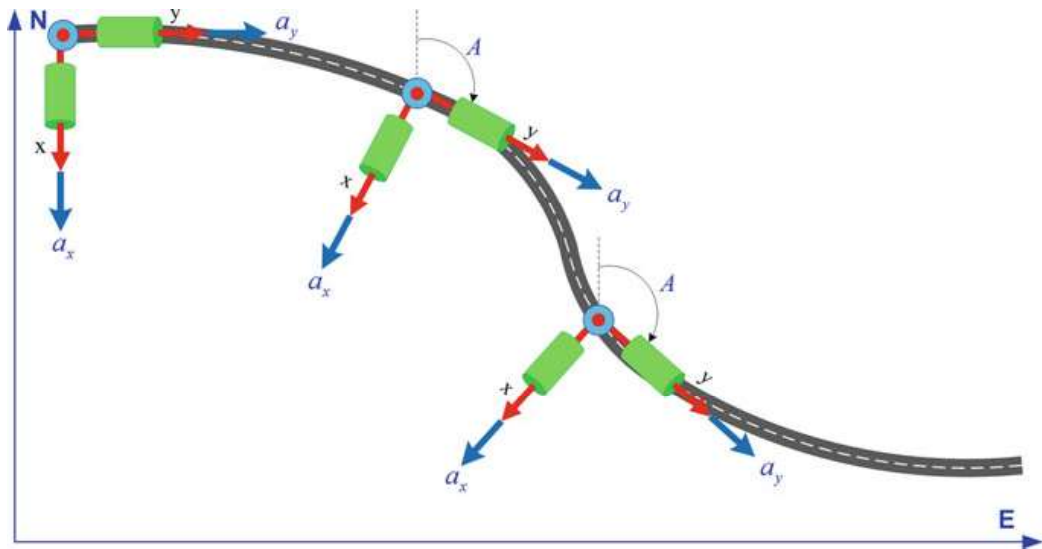


**Fig. 4.8** Inertial navigation using a 2D strapdown system

fixed coordinate frame. The stable Earth-fixed coordinate frame is often chosen as a local-level frame that is referred to as the navigation frame. As stated earlier, the transformation can either be established mechanically inside the INS by a stable platform or numerically as in the strapdown concept.

In 2D it is necessary to monitor both the translational motion of the vehicle in two directions and also its rotational motion, manifested as a change in direction. Two accelerometers are required to detect the acceleration in two directions. One gyroscope is required to detect the rotational motion in a direction perpendicular to the plane of motion (for simplicity, we neglect the Earth's rotation which would also be detected). Based on the advantages provided by a strapdown system, from this point on we shall limit our discussion to this type of system.

Strapdown systems mathematically transform the output of the accelerometers attached to the body into the east-north coordinate system (the 2D form of ENU) prior to performing the mathematical integration. These systems use the output of the gyroscope attached to the body to continuously update the transformation that is utilized to convert from body coordinates to east-north coordinates. Figure 4.8 shows the concept of inertial navigation in 2D as a platform makes turns, rotating through an angle  $A$  (called the azimuth angle<sup>1</sup>) measured from north. The blue cylindrical objects depict the accelerometers, the gyroscope is a blue disc whose sensitive axis depicted by a red dot points out of the paper towards the reader.

The accelerometers measure the acceleration of the body axes (X and Y) but we need the acceleration in the east-north coordinate system. This is accomplished using a transformation matrix which can be explained with the help of the diagram shown in Fig. 4.9.

<sup>1</sup> The terms azimuth angle and yaw angle are both used to represent the deviation from north. The difference lies in the direction of measurement: the azimuth angle is measured clockwise from north whereas the yaw angle is measured counter clockwise.

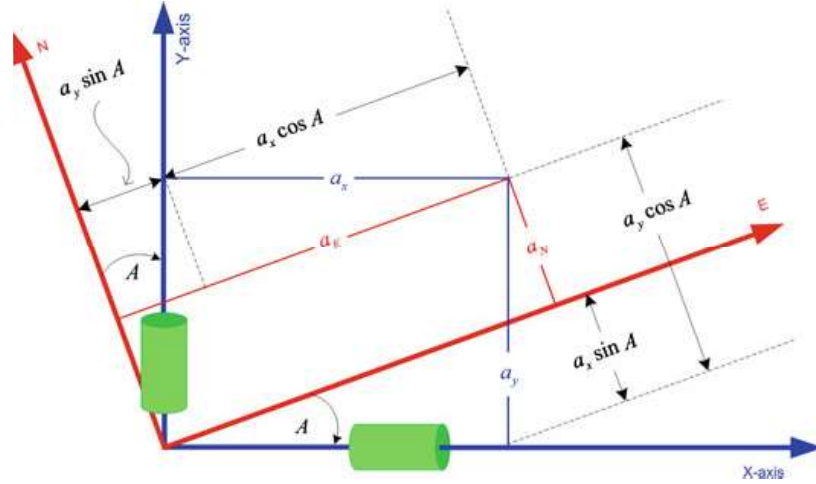


**Fig. 4.9** Transformation from the vehicle frame (X-Y) to the navigation frame (E-N)

The vehicle axes X and Y make an angle  $A$  with the east and north directions respectively, and the accelerations along east direction  $a_E$  and the north direction  $a_N$  can be written as

$$a_E = a_y \sin A + a_x \cos A \quad (4.13)$$

$$a_N = a_y \cos A - a_x \sin A \quad (4.14)$$

which in the matrix form is

$$\begin{bmatrix} a_E \\ a_N \end{bmatrix} = \begin{bmatrix} \cos A & \sin A \\ -\sin A & \cos A \end{bmatrix} \begin{bmatrix} a_x \\ a_y \end{bmatrix} \quad (4.15)$$

and can be expressed more compactly as

$$\mathbf{a}^n = R_b^n \mathbf{a}^b \quad (4.16)$$

where

$\mathbf{a}^n$  is the acceleration in the navigation frame (E-N)

$\mathbf{a}^b$  is the acceleration in the body frame measured by the accelerometers

$R_b^n$  is the rotation matrix which rotates  $\mathbf{a}^b$  to the navigation frame.

Given the accelerations in the navigation frame, we can integrate to obtain the velocities

$$\begin{aligned} v_E &= \int (a_x \cos A + a_y \sin A) dt \\ v_N &= \int (a_y \cos A - a_x \sin A) dt \end{aligned} \quad (4.17)$$

and again to obtain the position in the navigation frame

$$\begin{aligned} x_E &= \int \int (a_x \cos A + a_y \sin A) dt dt \\ x_N &= \int \int (a_y \cos A - a_x \sin A) dt dt \end{aligned} \quad (4.18)$$

which in the matrix form is

$$\begin{pmatrix} x_E \\ x_N \end{pmatrix} = \int \int \begin{pmatrix} \cos A & \sin A \\ -\sin A & \cos A \end{pmatrix} \begin{pmatrix} a_x \\ a_y \end{pmatrix} dt dt \quad (4.19)$$

It may be noted that this whole process is dependent on knowing the azimuth angle  $A$  which is calculated from the measurement by the gyroscope that monitors angular changes of the orientation of the accelerometers from the local E-N frame. These angular changes resolve the accelerometer measurements from the sensor axes into the local E-N axes. This angular change also determines the direction of motion of the moving platform defined by the azimuth angle, which is also known as the heading angle because it is the deviation from the north direction in the E-N plane. This is based on mathematically integrating the gyroscope angular velocity measurements relative to the initial azimuth angle  $A_0$  as follows

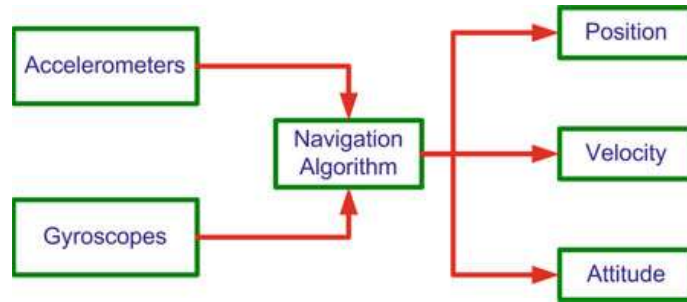
$$A(t) = \int \omega_{gyro} dt + A_0 \quad (4.20)$$

In this equation it should be noted (as pointed out previously) that the Earth's rotation components have been neglected for simplicity and ease of understanding of the basic concept of navigation.

## 4.6 Navigation in Three Dimensions

Inertial navigation in three dimensions (3D) requires three gyroscopes to measure the attitude angles of the body (pitch, roll and azimuth) and three accelerometers to measure accelerations along the three axes (in the east, north and up directions). Another complication is the involvement of gravity in the accelerations. The total acceleration encountered by the body is what is measured by the accelerometers, a combination of the acceleration due to gravity and that due to all other external forces. In order to remove the component of acceleration due to gravity, the tilt (or attitude) of the accelerometer with respect to the local vertical must be supplied by the gyroscope. At this point we will summarize the general concept of 3D inertial navigation. The mathematical details will be presented in a later chapter, where knowledge of 2D navigation will assist in understanding the subject.

**Fig. 4.10** The concept of inertial navigation



## 4.7 Overview of an Inertial Navigation System in 3D

The operation of an INS is based on processing the inertial sensor measurements received at its input and yielding a set of navigation parameters (position, velocity and attitude) of the moving platform at its output. In general these parameters are determined in a certain reference frame. Figure 4.10 shows the general concept of inertial navigation system.

The accelerometers are attached to the moving platform in order to monitor its accelerations in three mutually orthogonal directions. The gyroscopes provide the attitude (pitch, roll and azimuth) of the moving platform, and their measurements are used to rotate the data from the accelerometers into the navigation frame. The time integral of each acceleration component gives a continuous estimate of the corresponding velocity component of the platform relative to the initial velocities. A second integration yields the position with respect to a known starting point in a given frame of reference. This principle is outlined in Fig. 4.11.

## 4.8 Theoretical Measurements of the Inertial Sensor

Before delving into the details of inertial navigation and the errors associated with inertial sensors, it is important to look rather closely at the measurements taken by the accelerometer and gyroscope triads. To assist understanding, we will deal with the stationary and moving cases separately. Since the l-frame is more commonly used for everyday navigation (for reasons that will be described in Chap. 5) the ENU frame (a type of l-frame) will be used in this section where required.

### 4.8.1 Theoretical Measurements of a Stationary Accelerometer Triad

Consider the case where the accelerometer triad is stationary and level with the ground, as shown in Fig. 4.12. Since the accelerometers are stationary the only acting force will be the Earth's gravity (or more correctly the reaction to the force of gravity).

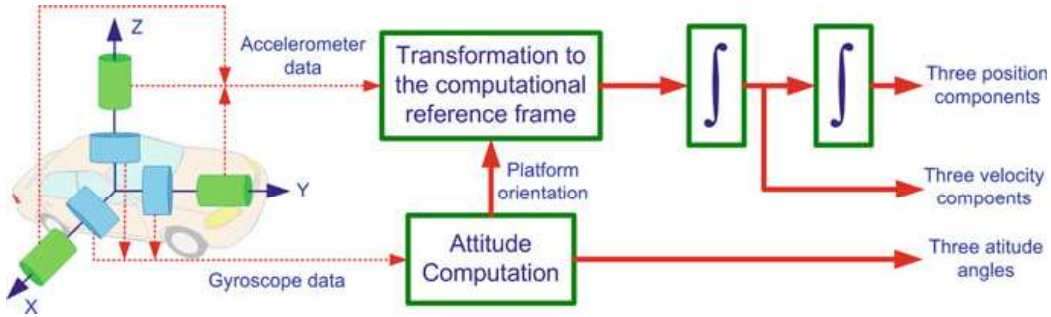
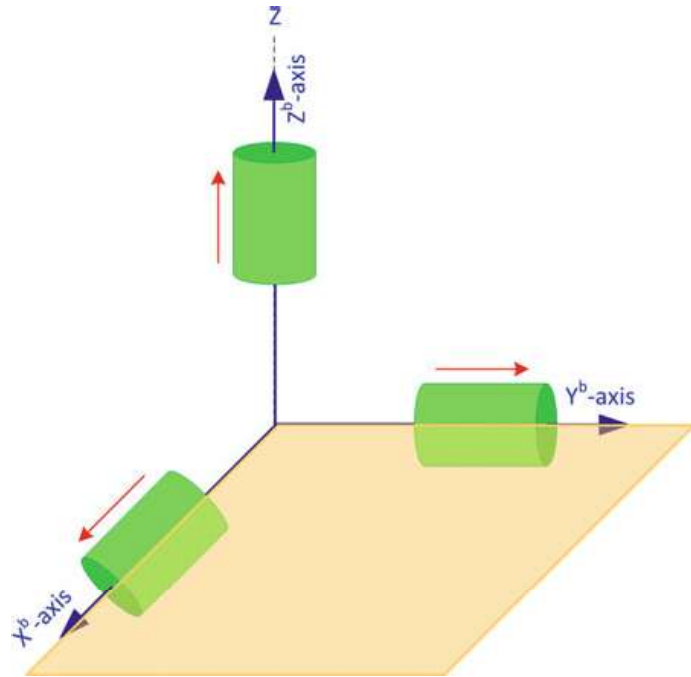


**Fig. 4.11** The general principle of inertial navigation in 3D

**Fig. 4.12** An accelerometer triad that is level with the ground



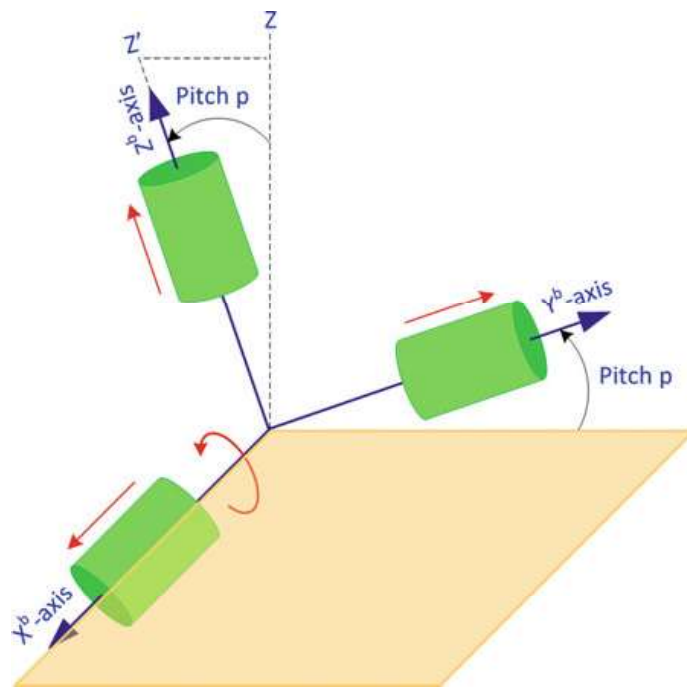
In this case the accelerometers pointing in the  $x$ ,  $y$  directions will not measure anything and the accelerometer in  $z$  direction measures the reaction to the gravity vector  $g$ . The nominal measurements will therefore be

$$f_x = 0; f_y = 0; f_z = g$$

It should be noted that the actual measurements will also have some errors (as we shall see later in Sect. 4.11.)

Now consider the case where the accelerometer triad is stationary but this time has been rotated about its  $x$ -axis to make an angle  $p$  with the ground, as shown in Fig. 4.13. As a consequence, the  $z$ -axis is inclined at the same angle from its previous position denoted as a dotted line  $Z$  into a new position shown as a dotted line  $Z'$ . As was defined in Chap. 2, the angle  $p$  is called the pitch angle. In this orientation, the accelerometers in the  $y$ ,  $z$  directions will each measure a portion of the gravity vector.

**Fig. 4.13** An accelerometer triad with the y-axis making an angle  $p$  (called pitch) with the level ground



According to the geometry of the Fig. 4.13, the measurements of the x and y accelerometers are

$$\begin{aligned} f_x &= 0 \\ f_y &= g \sin(p) \\ f_z &= g \cos(p) \end{aligned} \quad (4.21)$$

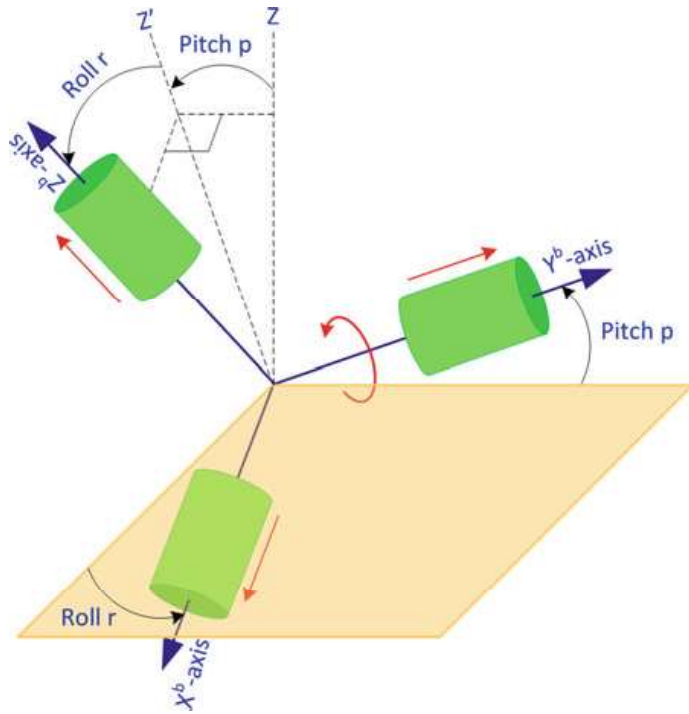
Now rotate the sensor triad about its y-axis so that its x-axis makes an angle  $r$  with its previous position and its z-axis makes the same angle  $r$  with its previous position  $Z'$ . This new orientation of the sensor triad is depicted in Fig. 4.14. In this orientation, all the accelerometers will be measuring some part of the gravity vector

$$\begin{aligned} f_x &= -g \cos(p) \sin(r) \\ f_y &= g \sin(p) \\ f_z &= g \cos(p) \cos(r) \end{aligned} \quad (4.22)$$

#### 4.8.2 Theoretical Measurements of a Stationary Gyro Triad

Now consider a gyroscope triad which is stationary on the Earth's surface. Since the triad is stationary, the only rotational motion acting on the sensors will be the Earth's rotation rate  $\omega_e$ . Now assume that the body frame (in this case is the triad

**Fig. 4.14** An accelerometer triad with the y-axis making an angle  $p$  (called pitch) with the level ground and with the y-axis then rotated through an angle  $r$  (called roll)



itself) coincides with the navigation frame, which is the ENU local-level frame, implying that

- x – axis: east
- y – axis: north
- z – axis: upward

as shown in Fig. 4.15.

In this stationary case the gyroscope measurements depend on the latitude of the gyro triad because they are merely measuring the Earth's rotation rate. Their measurements at the equator and at the poles will either be zero or  $\omega_e$ , depending on the direction of the sensitive axis of the gyroscope, but at any other point they will measure a quantity that lies between these limiting values in accordance with Table 4.2.

For an arbitrary point  $P$  on Earth and assuming that the b-frame is aligned with navigation frame, the measurements of the gyroscopes depend on latitude. This is depicted in Fig. 4.16.

According to Fig. 4.16, the components of the Earth's rotation measured by the gyro triad are

$$\omega_N = \omega_y = \omega_e \sin(90 - \varphi) = \omega_e \cos \varphi \quad (4.23)$$

$$\omega_U = \omega_z = \omega_e \cos(90 - \varphi) = \omega_e \sin \varphi \quad (4.24)$$

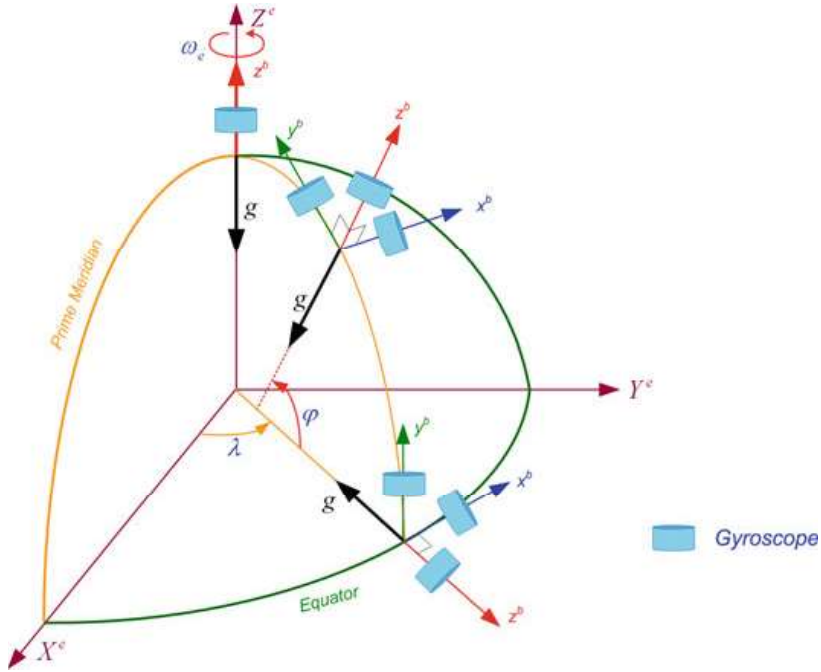


**Fig. 4.15** Gyroscope triad at the Earth's surface with its axis aligned with the ENU frame at latitudes 0, 90° and an arbitrary latitude in that range

**Table 4.2** The gyroscope measurements at various points on Earth

	Equator	Arbitrary position	North pole
$\omega_x$	0	0	0
$\omega_y$	$\omega_e$	$0-\omega_e$	0
$\omega_z$	0	$0-\omega_e$	$\omega_e$

and it is also evident that  $\omega_e = \sqrt{\omega_N^2 + \omega_U^2}$ . Also, because the x-gyro is located in a plane perpendicular to the Earth's rotation axis, it will not sense part of the Earth's rotation rate and hence  $\omega_E = 0$ .

These stationary measurements of the gyro triad represent the Earth's rotation interpreted in the local-level frame, denoted by the angular velocity vector  $\omega_{ie}^l$  as

$$\omega_{ie}^l = \begin{bmatrix} \omega_E \\ \omega_N \\ \omega_U \end{bmatrix} = \begin{bmatrix} 0 \\ \omega_e \cos \varphi \\ \omega_e \sin \varphi \end{bmatrix} \quad (4.25)$$

### 4.8.3 Theoretical Measurements of a Moving Gyro Triad

On a moving platform using the local-level frame as a navigation frame, the gyro triad will monitor two rotational components: the stationary part discussed in the previous section and the non-stationary part caused by the change of orientation of the local-level frame.

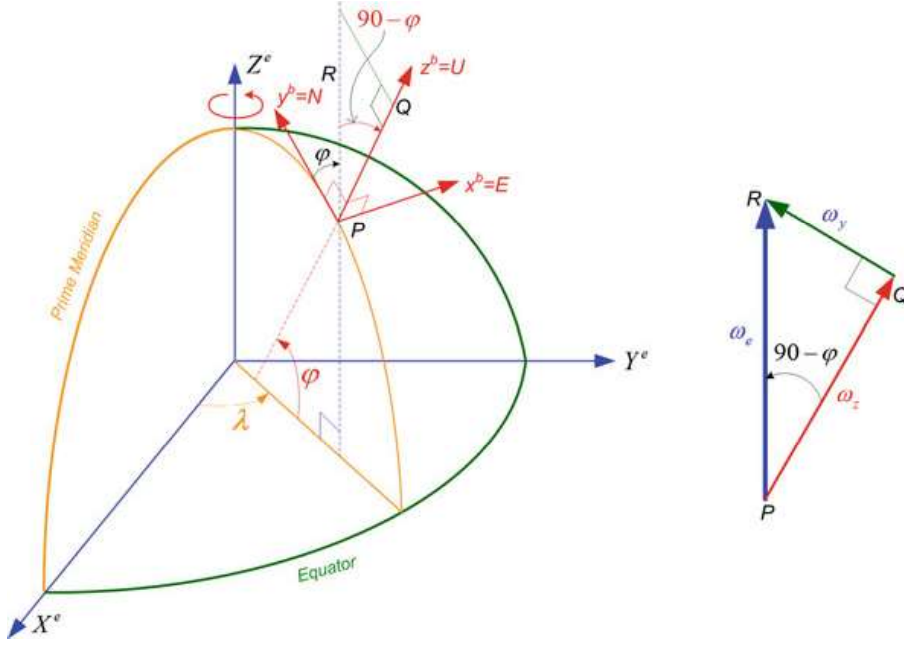


**Fig. 4.16** The geometry of the Earth's surface with a gyroscope triad at an arbitrary point P (in the ENU frame)

For simplicity, we will assume a vehicle that is moving with velocities  $v_e$  and  $v_n$  in the east and north directions respectively, and that the b-frame is aligned with the navigation frame. To generalize the measurement we will assume that the vehicle is moving across the Earth at an altitude  $h$ . In this case we will derive an expression for the rate of change of latitude  $\dot{\varphi}$  and longitude  $\dot{\lambda}$ .

Figure 4.17 shows the navigation frame (l-frame) as it moves over the surface of the Earth, viewed from the meridian plane.

The rate of change of the latitude  $\dot{\varphi}$  is

$$\frac{\Delta L_N}{\Delta t} = \frac{\Delta \varphi}{\Delta t} \times (R_M + h) \quad (4.26)$$

where  $\Delta L_N$  is the small segment of the arc covered during a small time  $\Delta t$ .

When  $\Delta t$  approaches zero

$$v_n = \dot{\varphi} \times (R_M + h) \quad (4.27)$$

$$\dot{\varphi} = \frac{v_n}{R_M + h} \quad (4.28)$$

Similarly, Fig. 4.18 shows the same l-frame as viewed from the top (z-axis) of the e-frame. Since the vehicle is moving in E-N, there will be a component of velocity along the east direction as well, and we can compute the rate of change of the longitude  $\dot{\lambda}$  as

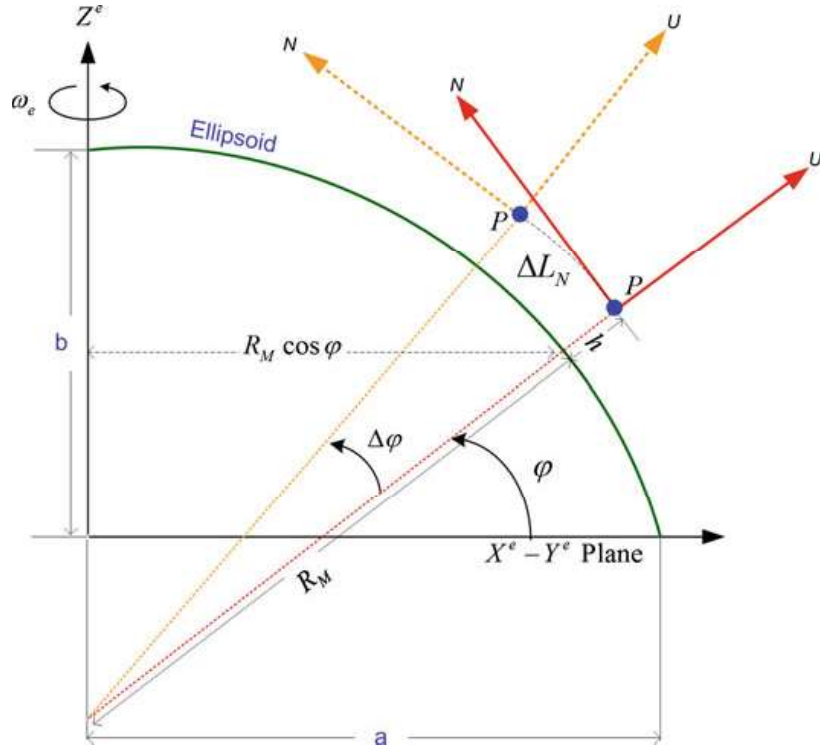


**Fig. 4.17** A depiction of the LLF as it moves over the Earth's surface, viewed from the meridian plane

$$\frac{\Delta L_E}{\Delta t} = \frac{\Delta \lambda}{\Delta t} \times (R_N + h) \cos \varphi \quad (4.29)$$

When  $\Delta t$  approaches zero

$$v_e = \dot{\lambda} \times (R_N + h) \cos \varphi \quad (4.30)$$

$$\dot{\lambda} = \frac{v_e}{(R_N + h) \cos \varphi} \quad (4.31)$$

and

$$\dot{h} = v_u \quad (4.32)$$

The gyroscopes of a moving triad will measure the stationary component due to the Earth's rotation as well the non-stationary component caused by the rate of change of latitude and longitude as the vehicle travels. According to the geometry of Fig. 4.16, the angular velocity of the local-level frame as measured by the gyroscope along the x-axis (the E direction) is

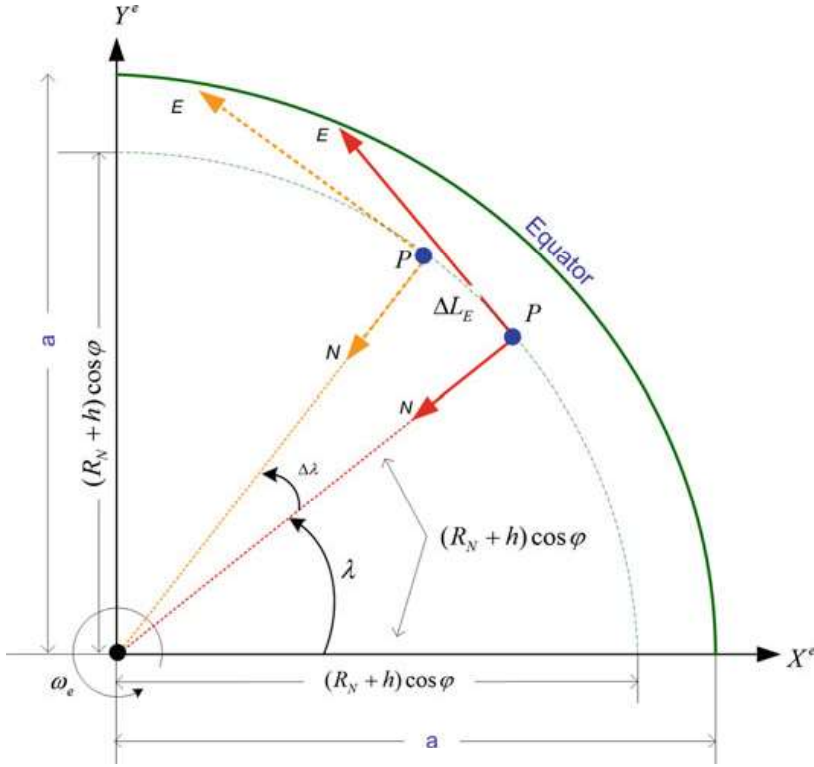


**Fig. 4.18** An illustration of the LLF over the Earth's surface, viewed from the z-axis

$$\omega_E = -\dot{\phi} = \underbrace{-\frac{v_n}{R_M + h}}_{\text{Non Stationary Component}} \quad (4.33)$$

and that for the y-axis (the N direction) is

$$\omega_N = \dot{\lambda} \cos \varphi + \omega^e \cos \varphi \quad (4.34)$$

Substituting  $\dot{\lambda}$  from Eq. (4.31) gives

$$\begin{aligned} \omega_N &= \frac{v_e}{(R_N + h) \cos \varphi} (\cos \varphi) + \omega^e \cos \varphi \\ \omega_N &= \underbrace{\frac{v_e}{R_N + h}}_{\text{Non Stationary Component}} + \underbrace{\omega^e \cos \varphi}_{\text{Stationary Component}} \end{aligned} \quad (4.35)$$

And the angular velocity measured by the gyroscope along the z-axis (the U direction) is

$$\begin{aligned}
\omega_U &= \dot{\lambda} \sin \varphi + \omega^e \sin \varphi \\
\omega_U &= \frac{v_e}{(R_N + h) \cos \varphi} \sin \varphi + \omega^e \sin \varphi \\
\omega_U &= \underbrace{\frac{v_e}{R_N + h} \tan \varphi}_{\text{Non Stationary Component}} + \underbrace{\omega^e \sin \varphi}_{\text{Stationary Component}}
\end{aligned} \tag{4.36}$$

The angular velocity of the local-level frame with respect to the e-frame as expressed in the local level frame  $\omega_{el}^l$  consists of the non-stationary components

$$\boldsymbol{\omega}_{el}^l = \begin{bmatrix} \omega_E \\ \omega_N \\ \omega_U \end{bmatrix}_{\text{Non-stationary component}} = \begin{bmatrix} -\dot{\varphi} \\ \dot{\lambda} \cos \varphi \\ \dot{\lambda} \sin \varphi \end{bmatrix} = \begin{bmatrix} -\frac{v_n}{R_M + h} \\ \frac{v_e}{R_N + h} \\ \frac{v_e \tan \varphi}{R_N + h} \end{bmatrix} \tag{4.37}$$

## 4.9 Notes on Inertial Sensor Measurements

In the examples above, it was assumed that the INS body frame was aligned with the navigation frame. But for strapdown systems the b-frame can take essentially any arbitrary direction because the accelerometers and gyros are strapped onto the vehicle, which can adopt any orientation with respect to the navigation frame. The establishment of the relationship between the INS body frame and the local level (navigation) frame is usually done at the beginning of the survey by a stationary alignment process. If continuous external velocity information is available (e.g. from GPS) this can be done in kinematic mode. In this process, the initial attitude angles (pitch, roll and azimuth) between the b-frame and the n-frame require to be estimated. The attitude angles are used in generating the rotation matrix  $R_b^n$  for the transformation from the b-frame to the n-frame. The rotation rates measured by the gyros are used to constantly update this matrix. Once this transformation has been made, the process of integrating an acceleration measurement twice will provide the IMU's position difference relative to the initial point.

However, as noted earlier, accelerometers cannot separate the total platform acceleration from that caused by the presence of gravity. In fact, accelerometers provide the sum of the platform's acceleration in space and its acceleration due to gravity. The accelerometer measurements must be combined with knowledge of the ambient gravitational field in order to determine the acceleration of the vehicle with respect to a non-inertial reference frame. Obviously, the inertial navigation is fundamentally dependent on an accurate specification of the position, velocity and attitude of the moving platform prior to the start of navigation.

## 4.10 Inertial Sensor Performance Characteristics

To assess an inertial sensor for a particular application, numerous characteristics must be considered. But first we will introduce some general terms.

- a. **Repeatability:** The ability of a sensor to provide the same output for repeated applications of the same input, presuming all other factors in the environment remain constant. It refers to the maximum variation between repeated measurements in the same conditions over multiple runs.
- b. **Stability:** This is the ability of a sensor to provide the same output when measuring a constant input over a period of time. It is defined for single run.
- c. **Drift:** The term drift is often used to describe the change that occurs in a sensor measurement when there is no change in the input. It is also used to describe the change that occurs when there is zero input.

The performance characteristics of inertial sensors (either accelerometers or gyroscopes) are usually described in terms of the following principal parameters: sensor bias, sensor scale factor, noise and bandwidth. These parameters (among others) will be discussed in the next section, which deals with the errors of inertial sensors.

## 4.11 Inertial Sensor Errors

Inertial sensors are prone to various errors which get more complex as the price of the sensor goes down. The errors limit the accuracy to which the observables can be measured. They are classified according to two broad categories of systematic and stochastic (or random) errors.

### 4.11.1 Systematic Errors

These types of errors can be compensated by laboratory calibration, especially for high-end sensors. Some common systematic sensor errors (Grewal et al. 2007) are described below.

#### 4.11.1.1 Systematic Bias Offset

This is a bias offset exhibited by all accelerometers and gyros. It is defined as the output of the sensor when there is zero input, and is depicted in Fig. 4.19. It is independent of the underlying specific force and angular rate.

**Fig. 4.19** Inertial sensor bias error

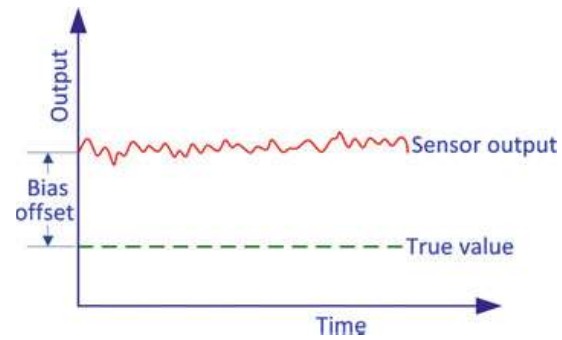
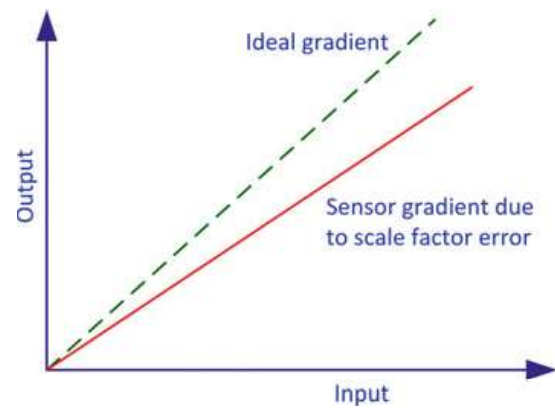


**Fig. 4.20** Inertial sensor scale factor error



#### 4.11.1.2 Scale Factor Error

This is the deviation of the input–output gradient from unity. The accelerometer output error due to scale factor error is proportional to the true specific force along the sensitive axis, whereas the gyroscope output error due to scale factor error is proportional to the true angular rate about the sensitive axis. Figure 4.20 illustrates the effect of the scale factor error.

#### 4.11.1.3 Non-linearity

This is non-linearity between the input and the output, as shown in Fig. 4.21.

#### 4.11.1.4 Scale Factor Sign Asymmetry

This is due to the different scale factors for positive and negative inputs, as shown in Fig. 4.22.

**Fig. 4.21** Non-linearity of inertial sensor output

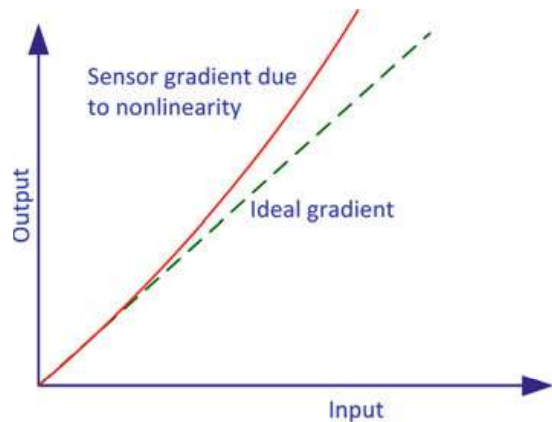


**Fig. 4.22** Scale factor sign asymmetry

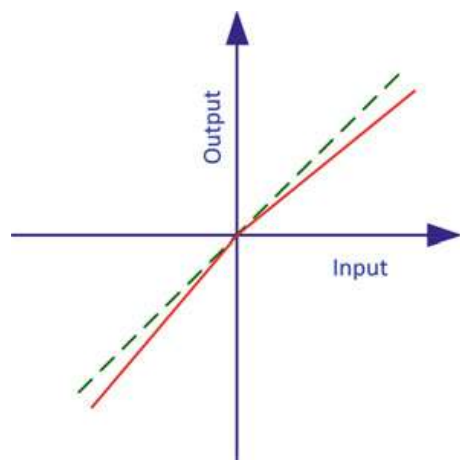
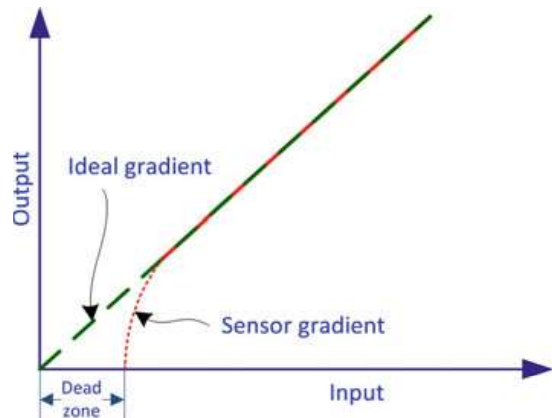


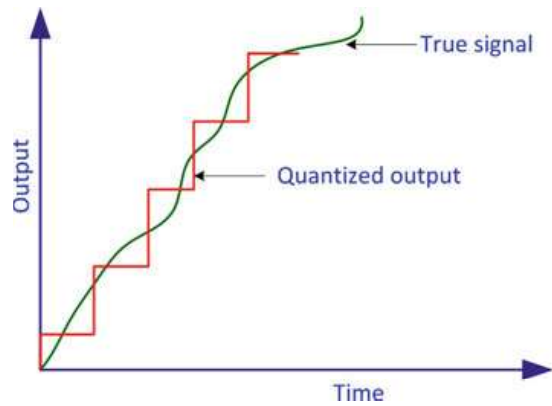
**Fig. 4.23** Dead zone in the output of an inertial sensor



#### 4.11.1.5 Dead Zone

This is the range where there is no output despite the presence of an input, and it is shown in Fig. 4.23.

**Fig. 4.24** The error due to quantization of an analog signal to a digital signal



#### 4.11.1.6 Quantization Error

This type of error is present in all digital systems which generate their inputs from analog signals, and is illustrated in Fig. 4.24.

#### 4.11.1.7 Non-orthogonality Error

As the name suggests, non-orthogonality errors occur when any of the axes of the sensor triad depart from mutual orthogonality. This usually happens at the time of manufacturing. Figure 4.25 depicts the case of the z-axis being misaligned by an angular offset of  $\theta_{zx}$  from xz-plane and  $\theta_{zy}$  from the yz-plane.

#### 4.11.1.8 Misalignment Error

This is the result of misaligning the sensitive axes of the inertial sensors relative to the orthogonal axes of the body frame as a result of mounting imperfections. This is depicted in Fig. 4.26 for a sensor frame misalignment (using superscript ‘s’) with respect to the body in a 2D system in which the axes are offset by the small angle  $\delta\theta$ .

### 4.11.2 Random Errors

Inertial sensors suffer from a variety of random errors which are usually modeled stochastically in order to mitigate their effects.

**Fig. 4.25** Sensor axes non-orthogonality error

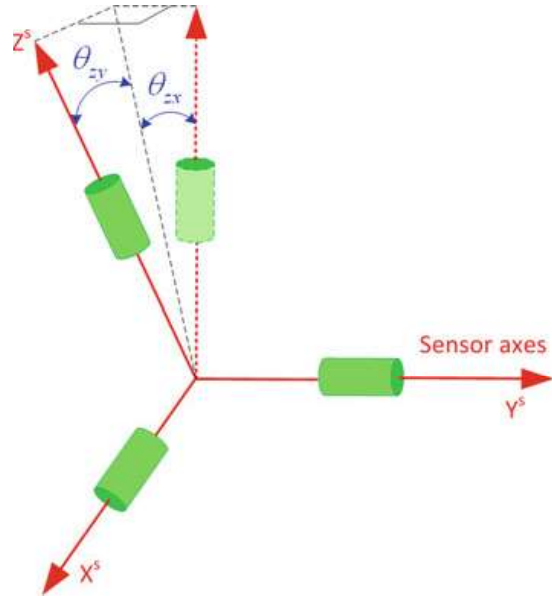
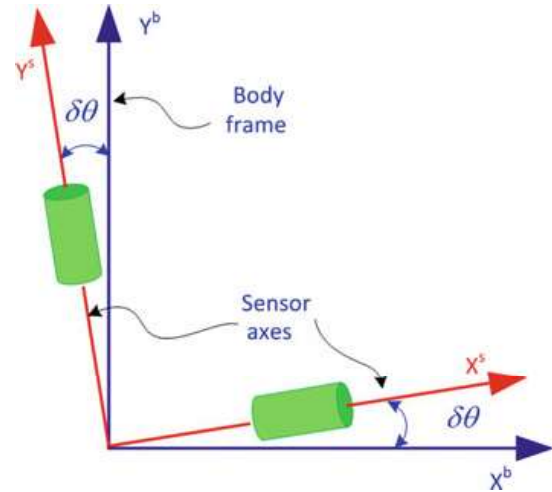


**Fig. 4.26** Misalignment error between the body frame and the sensor axes



#### 4.11.2.1 Run-to-Run Bias Offset

If the bias offset changes for every run, this falls under the bias repeatability error, and is called the run-to-run bias offset.

#### 4.11.2.2 Bias Drift

This is a random change in bias over time during a run. It is the instability in the sensor bias for a single run, and is called bias drift. It is illustrated in Fig. 4.27. Bias is deterministic but bias drift is stochastic. One cause of bias drift is a change in temperature.

**Fig. 4.27** Error in sensor output due to bias drift

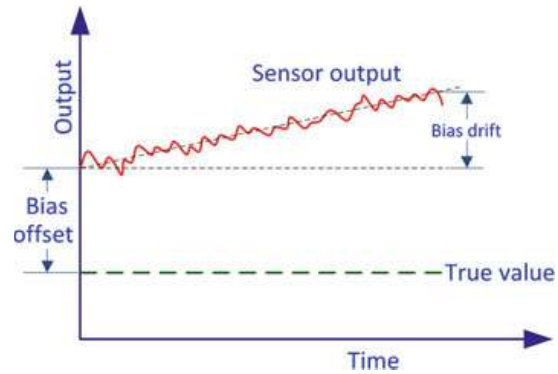
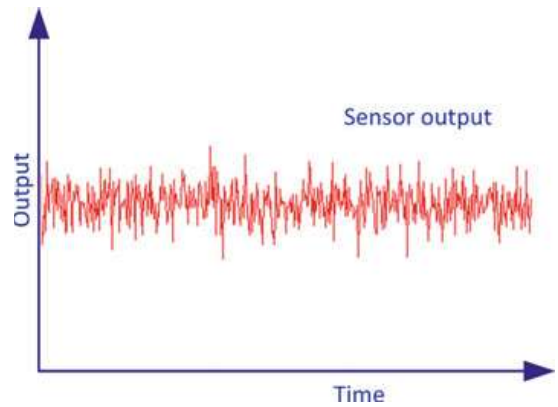


**Fig. 4.28** A depiction of white noise error



#### 4.11.2.3 Scale Factor Instability

Random changes in scale factor during a single run. This is usually the result of temperature variations. The scale factor can also change from run to run, but stay constant during a particular run. This demonstrates the repeatability of the sensor and is also called the run-to-run scale factor.

#### 4.11.2.4 White Noise

This is an uncorrelated noise that is evenly distributed in all frequencies. This type of noise can be caused by power sources but can also be intrinsic to semiconductor devices. White noise is illustrated in Fig. 4.28.

### 4.11.3 Notes on Random Errors

Most manufacturers express the randomness associated with their inertial sensors by the concept of random walk. The angle random walk (ARW) for gyroscopes is usually specified in terms of  $\text{deg}/\text{hr}/\sqrt{\text{Hz}}$  or  $\text{deg}/\sqrt{\text{hr}}$ , and the velocity random

**Table 4.3** Performance specification of various KVH gyroscopes

	KVH DSP-300 (single axis FOG)	KVH DSP-3100 (single axis FOG)	DSP-3400 single axis FOG
Bandwidth	100 Hz	1000 Hz	1000 Hz
Bias drift	<3°/h	<1°/h	<1°/h
ARW	<6°/h/ $\sqrt{\text{Hz}}$ $(0.1^\circ/\sqrt{\text{h}})$	<4°/h/ $\sqrt{\text{Hz}}$ $(0.0667^\circ/\sqrt{\text{h}})$	<4°/h/ $\sqrt{\text{Hz}}$ $(0.0667^\circ/\sqrt{\text{h}})$
Scale factor	<0.05 %	<0.05 %	<0.05 %

walk (VRW) for accelerometers is given in terms of  $\mu\text{g}/\sqrt{\text{Hz}}$  or  $\text{m/s}/\sqrt{\text{hr}}$ . This definition requires knowledge of the data rate (sampling frequency) at which the sensor measurements are acquired by the data acquisition systems. The data rate is related to the bandwidth of the sensor, which is another important parameter. The inertial sensor bandwidth (specified in Hz) defines the range of frequencies that can be monitored by the sensor. For example a gyroscope with 100 Hz bandwidth is capable of monitoring the dynamics of frequencies less than 100 Hz. Any higher frequencies will not be detected. For this, the sensor has to sample the signal with at least double the maximum frequency; in this case 200 Hz. But whilst increasing the data rate will broaden the bandwidth to facilitate monitoring higher frequency dynamics, the measurements will also be noisier. Table 4.3 shows some important performance specifications for various KVH gyroscopes (KVH 2012).

#### 4.11.4 Mathematical Models of Inertial Sensor Errors

The performance of an INS can be described in terms of its two major groups of sensors, namely gyroscopes and accelerometers.

##### 4.11.4.1 Gyroscope Measurement Model

Gyroscopes are angular rate sensors that provide either angular rate or attitude depending on whether they are of the rate sensing or rate integrating type.

Measurements of angular rate can be modeled by the observation equation

$$\tilde{\omega}_{ib}^b = \omega_{ib}^b + \mathbf{b}_g + S\omega_{ib}^b + N\omega_{ib}^b + \boldsymbol{\varepsilon}_g \quad (4.38)$$

where

- $\tilde{\omega}_{ib}^b$  is the gyroscope measurement vector (deg/h)
- $\omega_{ib}^b$  is the true angular rate velocity vector (deg/h)

- $\mathbf{b}_g$  is the gyroscope instrument bias vector (deg/h)
- $S_g$  is a matrix representing the gyro scale factor
- $N_g$  is a matrix representing non-orthogonality of the gyro triad
- $\boldsymbol{\epsilon}_g$  is a vector representing the gyro sensor noise (deg/h).

The matrices  $N_g$  and  $S_g$  are given as

$$N_g = \begin{bmatrix} 1 & \theta_{g,xy} & \theta_{g,xz} \\ \theta_{g,yx} & 1 & \theta_{g,yz} \\ \theta_{g,zx} & \theta_{g,zy} & 1 \end{bmatrix}$$

$$S_g = \begin{bmatrix} s_{g,x} & 0 & 0 \\ 0 & s_{g,y} & 0 \\ 0 & 0 & s_{g,z} \end{bmatrix}$$

where  $\theta_{(.,.)}$  are the small angles defining the misalignments between the different gyro axes and  $s_{(.,.)}$  are the scale factors for the three gyros.

#### 4.11.4.2 Accelerometer Measurement Model

Performance factors describing accelerometer accuracy are similar to those which characterize the gyro accuracy bias uncertainty, scale factor stability, and random noise. Measurements of the specific force can be modeled by the observation equation

$$\tilde{\mathbf{f}}^b = \mathbf{f}^b + \mathbf{b}_a + \mathbf{S}_1 \mathbf{f} + \mathbf{S}_2 \mathbf{f}^2 + \mathbf{N}_a \mathbf{f} + \delta \mathbf{g} + \boldsymbol{\epsilon}_a \quad (4.39)$$

where

- $\tilde{\mathbf{f}}^b$  is the accelerometer measurement vector ( $\text{m/s}^2$ )
- $\mathbf{f}^b$  is the true specific force vector (i.e. observable) ( $\text{m/s}^2$ )
- $\mathbf{b}_a$  is the accelerometer instrument bias vector ( $\text{m/s}^2$ )
- $S_1$  is a matrix of the linear scale factor error
- $S_2$  is a matrix of the non-linear scale factor error
- $N_a$  is a matrix representing non-orthogonality of the accelerometer triad
- $\delta \mathbf{g}$  is the anomalous gravity vector (i.e. the deviation from the theoretical gravity value) ( $\text{m/s}^2$ )
- $\boldsymbol{\epsilon}_a$  is a vector representing the accelerometer sensor noise ( $\text{m/s}^2$ ).

The matrices  $N_a$ ,  $S_1$  and  $S_2$  are

$$N_a = \begin{bmatrix} 1 & \theta_{a,xy} & \theta_{a,xz} \\ \theta_{a,yx} & 1 & \theta_{a,yz} \\ \theta_{a,zx} & \theta_{a,zy} & 1 \end{bmatrix}$$

**Table 4.4** Classification of inertial measurement units

Performance	Strategic grade	Navigation grade	Tactical grade	Commercial grade <sup>a</sup>
Positional error	30 m/ h < 100 m/h	1 nmi <sup>b</sup> /h or .5 m/s	10–20 nmi/h	Large variation
Gyroscope drift	0.0001–0.001	<0.01 °/h	1–10°/h	0.1°/s
Gyroscope random walk	–	<0.002°/√h	0.05– <0.02°/√h	Several °/√h
Accelerometer bias	0.1–1	<100 μg	1–5 mg	100–1,000 μg
Applications	Submarines Intercontinental ballistic missile	General navigation high precision georeferencing mapping	Integrated with GPS for mapping Weapons (short time))	Research Low cost navigation pedometers, Antilock breaking active suspension, airbags

<sup>a</sup> Also called automotive grade<sup>b</sup> 1 nautical mile (nmi) ≈ 6,076 ft ≈ 1,851 m

$$S_1 = \begin{bmatrix} s_{1,x} & 0 & 0 \\ 0 & s_{1,y} & 0 \\ 0 & 0 & s_{1,z} \end{bmatrix}$$

$$S_2 = \begin{bmatrix} s_{2,x} & 0 & 0 \\ 0 & s_{2,y} & 0 \\ 0 & 0 & s_{2,z} \end{bmatrix}$$

where  $\theta_{(.,.)}$  are the small angles defining the misalignments between the different accelerometer axes and  $s_{(.,.)}$  are the scale factors for the three accelerometers.

For both the inertial sensors, the scale factors and biases are usually considered to be constant (over a certain time) but unknown quantities which are uncorrelated between the different sensors. In principle these errors can be eliminated by the calibration techniques described in Sect. 4.13. The sensor noise  $\varepsilon$  consists of white noise, correlated noise and random walk, etc. In principle these errors can be minimized by the estimation techniques described in Chap. 7.

## 4.12 Classification of Inertial Sensors

No universally agreed definition exists for categorizing inertial sensors. However, a rough comparison of different inertial navigation sensors/systems is outlined in Table 4.4 with data obtained from (Groves Dec 2007), (Petovello et al. Jun 2007), (Barbour and Schmidt 2001) and (Wang and Williams 2008).

Usually the cost of an IMU is dictated by the type of inertial sensors. IMUs are categorized according to their intended applications, which mainly depend on the gyroscope bias expressed in deg/hour. A secondary measure of performance is the gyroscope random walk, which is usually expressed in terms of deg/root-hour and accelerometer bias.

### ***4.12.1 Gyroscope Technologies and their Applications***

There are several gyroscope technologies, including ring laser gyroscopes (RLG), dynamically tuned gyroscopes (DTG), hemispherical resonant gyroscopes (HRG), and interferometric fiber-optic gyroscopes (IFOG). Spinning mass and ring laser gyroscopes offer high performance but at high cost, and find their application in strategic/tactical and submarine navigation systems. DTG offer a medium level of performance and share some applications with RLG (Prasad and Ruggieri 2005). IFOG and Coriolis-based gyroscopes are of lower performance but cost less and are typically used in torpedoes, tactical missile midcourse guidance, flight control and smart munitions guidance and robotics. There has been a recent trend towards MEMS gyroscopes that are being researched for low cost navigation applications such as car navigation and portable navigation devices. Details of all these sensor technologies can be found in (Barbour and Schmidt 2001; Lawrence 1998).

### ***4.12.2 Accelerometer Technologies and their Applications***

The main accelerometer technologies are mechanical pendulous force-rebalance accelerometers, vibrating beam accelerometers (VBAs) and gravimeters. The best performance is provided by mechanically floated instruments, and these are used in strategic missiles. Mechanical pendulous rebalance accelerometers are used in submarine navigation, land and aircraft navigation and space applications. Quartz resonator accelerometers are low grade sensors typically found in tactical missile midcourse guidance.

## **4.13 Calibration of Inertial Sensors**

Calibration is defined as the process of comparing instrument outputs with known reference information to determine coefficients that force the output to agree with the reference information across the desired range of output values. Calibration is used to compute deterministic errors of sensors in the laboratory. The calibration parameters to be determined can change according to the specific technology in an IMU. To accurately determine all of the parameters, special calibration devices are

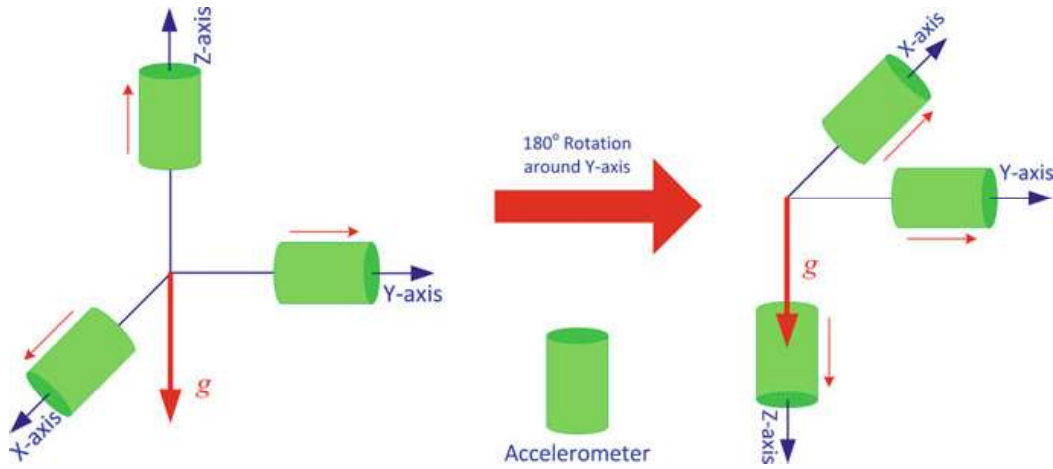


**Fig. 4.29** Calibrating an accelerometer, with the sensitive axis facing upward on the *left* and downward on the *right*

needed, such as three-axial turntables, to perform either a six-position static test or an angle rate test.

### 4.13.1 Six-Position Static Test

In this procedure for sensor calibration, the inertial system is mounted on a level table with each sensitive axis pointing alternately up and down (six positions for three axes). Using these sensor readings it is possible to extract estimates of the accelerometer bias and scale factor by summing and differencing combinations of the inertial system measurements.

#### 4.13.1.1 Accelerometer Calibration

Accelerometers are normally calibrated by sensing gravity. Each accelerometer of the triad is placed on a calibrated rate table with its sensitive axis facing up. After taking about 10–15 min of data, the mean  $f_{up}$  is computed. Then a similar reading is taken for  $f_{down}$  with sensitive axis pointed downwards. To reiterate the point made earlier, the accelerometers will measure the reaction to gravity.

By Fig. 4.29, the measurements with the sensitive axis of the accelerometer up and down can be expressed as

$$f_{up} = b_a + (1 + S_a)g \quad (4.40)$$

$$f_{down} = b_a - (1 + S_a)g \quad (4.41)$$

The bias  $b_a$  is computed by adding these two reading

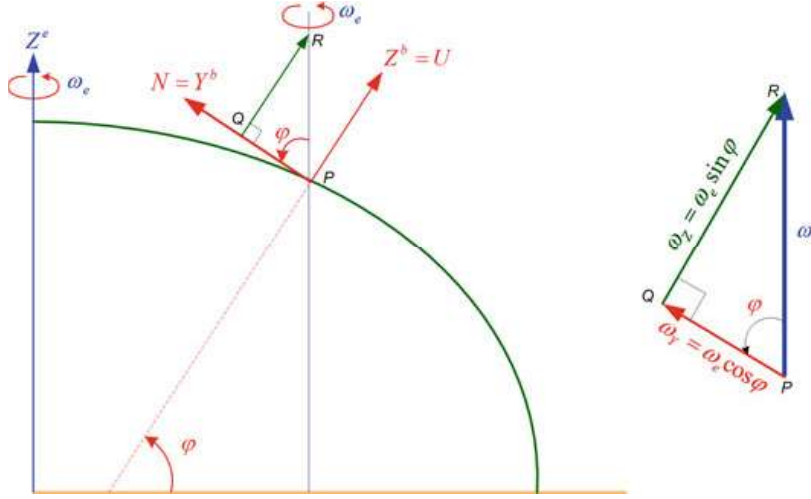


**Fig. 4.30** Geometry explaining the component of the Earth's rotation measured by gyros aligned with the north and up directions

$$b_a = \frac{f_{up} + f_{down}}{2} \quad (4.42)$$

and the scale factor  $S_a$  is obtained by subtracting the two reading

$$S_a = \frac{f_{up} - f_{down} - 2g}{2g} \quad (4.43)$$

where  $g$  represents gravity.

This procedure is repeated for each of the three accelerometers to obtain their individual bias and scale factors.

#### 4.13.1.2 Gyroscope Calibration

A similar procedure is employed for gyroscopes, but this time the Earth's rotation rate is measured instead of gravity. According to Fig. 4.30, for a body frame located at a latitude  $\varphi$  the theoretical projections of the Earth's rotation rate on the body axes are

$$\omega_x = 0; \omega_y = \omega_e \cos \varphi; \omega_z = \omega_e \sin \varphi$$

Therefore, a vertical gyroscope (with its sensitive axis pointing up) will sense a component of gravity that is  $\omega_e \sin \varphi$ , and this is used in the calibration.

In accordance with Fig. 4.31, the measurements of the gyroscope with its sensitive axis up and down are

$$\omega_{up} = b_{go} + (1 + S_g)\omega_e \sin \varphi \quad (4.44)$$

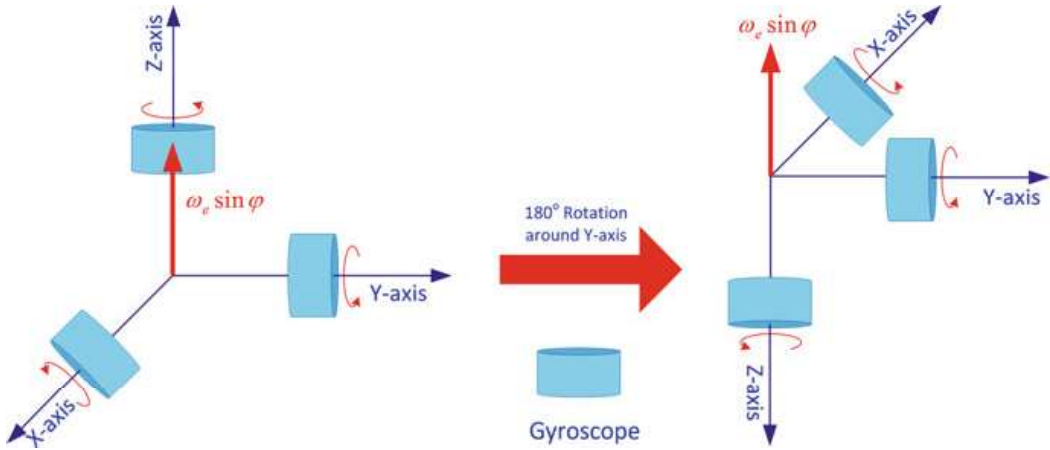


**Fig. 4.31** Calibrating a gyroscope, with the sensitive axis facing upward on the *left* and downward on the *right*

$$\omega_{down} = b_{gyo} - (1 + S_g)\omega_e \sin \varphi \quad (4.45)$$

where  $\omega_e \sin \varphi$  is the vertical component of the Earth's rotation rate,  $\omega_e$  is the Earth's rotation rate about its spin axis, and  $\varphi$  is the latitude of the location of the gyroscope.

The bias and scale factor are obtained in a similar way as for accelerometers

$$b_g = \frac{\omega_{up} + \omega_{down}}{2} \quad (4.46)$$

$$S_g = \frac{\omega_{up} - \omega_{down} - 2\omega_e \sin \varphi}{2\omega_e \sin \varphi} \quad (4.47)$$

where  $b_{gyro}$  is the bias,  $S_{gyro}$  is the scale factor,  $\omega_e$  is the Earth's rotation rate and  $\varphi$  is the latitude of the location of the gyroscope.

This procedure is repeated for each of the three gyroscopes to obtain their individual bias and scale factors.

For low cost gyroscopes that cannot detect the Earth's rotation rate, the table can be rotated at a constant rate of  $\omega_t = 60^\circ/\text{s}$  (or any indeed other rate that is above the detection threshold of the gyroscopes) and  $\omega_e \sin \varphi$  is replaced with the value of  $\omega_t$  in Eqs. (4.44), (4.45) and (4.47).

### 4.13.2 Angle Rate Tests

Angle rate tests are utilized to calibrate gyroscope biases, scale factors and non-orthogonalities. In this type of calibration the IMU is mounted on a precision rate table (Fig. 4.32 shows one) which is rotated through a set of very accurately defined angles. By comparing these known rotations with the estimates of the

**Fig. 4.32** A precision rate table with a gyroscope mounted on top

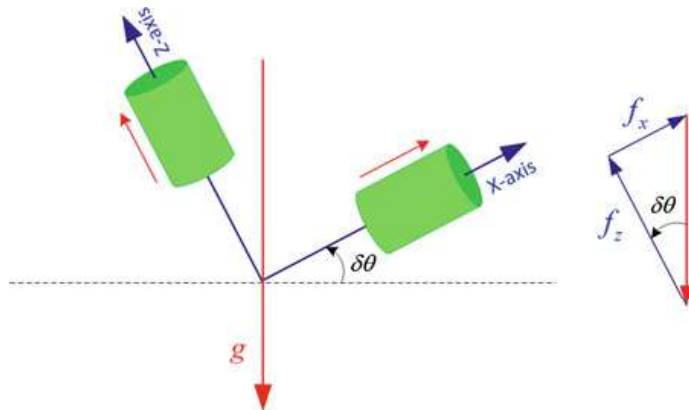


angles obtained by integrating the rate outputs provided by the gyros, it is possible to estimate the various errors in the gyros measurements. For instance, if the table is rotated clockwise and counterclockwise through the same angle then the biases and scale factors errors of the gyros can be estimated.

#### 4.14 Importance of Calibration of Inertial Sensors

Calibration of the inertial sensors plays an important role in the ultimate accuracy of an INS. Any residual flaws in the sensors cause errors which, as we shall see, tend to grow with time.

**Fig. 4.33** A stationary accelerometer placed on a tilted plane



Consider Fig. 4.33, which shows a stationary accelerometer on a plane tilted from horizontal by the small angle  $\delta\theta$ . We can prove that this tilt is observable because the accelerometers are sitting in a gravitational field.

The accelerometers will measure a component of  $g$  as follows

$$f_z = g \cos \delta\theta \text{ in the } z \text{ direction} \quad (4.48)$$

$$f_x = g \sin \delta\theta \text{ in the } x \text{ direction} \quad (4.49)$$

where  $g$  is the magnitude of the gravitational field.

For small angles where  $\cos \delta\theta$  is near unity and  $\sin \delta\theta$  is  $\delta\theta$ , the measured values can be approximated as

$$f_z = g \quad (4.50)$$

$$f_x = g\delta\theta \quad (4.51)$$

Therefore the output of the  $x$  accelerometer gives us a direct measurement of the tilt about the  $y$  axis. Similarly, the output of the  $y$  accelerometer provides a measure of the tilt about the  $x$  axis. This discussion provides a simple example on correlation of errors. If the  $x$  accelerometer has a bias error of  $b_x$ , the output of the accelerometer will be

$$f_x = b_x + g\delta\theta \quad (4.52)$$

If we are trying to level the platform (which involves determining its attitude because we do not actually rotate the sensors in a strapdown system) employing the accelerometer output, we cannot tell the difference between the contribution of accelerometer bias or the tilt. Hence, the value of the sensor bias determines the accuracy to which we can estimate the initial tilt alignment of the INS (as will be discussed in greater detail later). This can be clearly explained in the case of small tilt angles where  $f_x$  will be approximately zero and

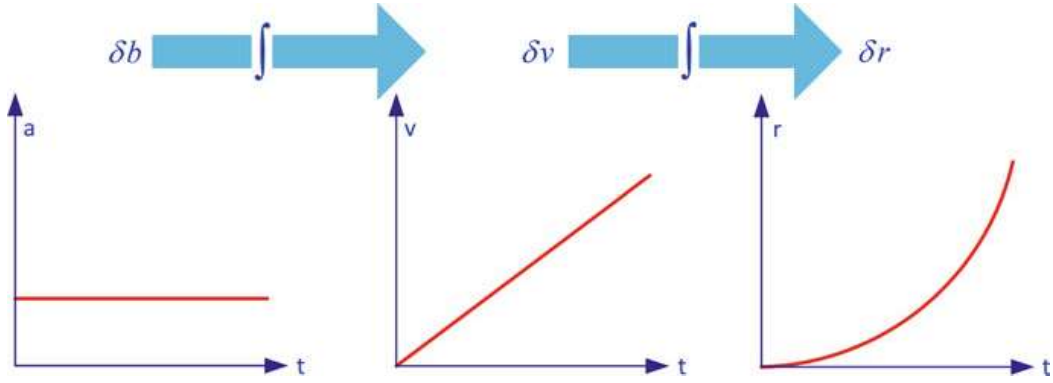


**Fig. 4.34** Effect of a bias error in acceleration, velocity and position

$$\delta\theta \approx -\frac{b_x}{g} \quad (4.53)$$

#### 4.14.1 Case-I: Bias Error in an Accelerometer

An uncompensated accelerometer bias error  $b_f$  (expressed in terms of either g or  $\text{m/s}^2$ ) will introduce an error proportional to  $t$  in the velocity measurement and an error proportional to  $t^2$  in the position measurement due to the integrations to obtain the velocity  $v$  and the position  $r$  from the gyroscope output. Taking these into account

$$v = \int b_f dt \quad (4.54)$$

$$r = \int v dt = \int \int b_f dt = \frac{1}{2} b_f t^2 \quad (4.55)$$

Therefore an accelerometer bias introduces a first-order error in velocity and a second-order error in the position, as shown in Fig. 4.34.

#### 4.14.2 Case-II: Bias Error in the Gyroscope

An uncompensated gyro bias (expressed in terms of deg/h or radians/s) in the gyro error  $b_\omega$  will introduce an angle error (in roll or pitch) that is proportional to time  $t$ , and hence

$$\delta\theta = \int b_\omega dt = b_\omega t \quad (4.56)$$

This misalignment of the INS will result in the measured acceleration vector being incorrectly projected. This in turn will introduce acceleration in one of the horizontal channels (as mentioned previously) with a value of

$$a = g \sin(\delta\theta) \approx g\delta\theta \approx gb_\omega t \quad (4.57)$$

Now when we integrate this acceleration to obtain the velocity and position, it will introduce an error proportional to  $t^2$  in the velocity of

$$v = \int b_\omega g t dt = \frac{1}{2} b_\omega g t^2 \quad (4.58)$$

and an error proportional to  $t^3$  in the position of

$$r = \int v dt = \int \int \frac{1}{2} b_\omega g t^2 dt = \frac{1}{6} b_\omega g t^3 \quad (4.59)$$

Since, a gyro bias introduces a second-order error in velocity and a third-order error in position, the gyroscope tends to dictate the quality of an IMU and thus the accuracy of the output of navigation algorithms.

## 4.15 Initialization and Alignment of Inertial Sensors

An INS takes acceleration and rotation rates from sensors to calculate velocity and attitudes by integrating them once, and then integrates the velocity in order to obtain the position. The navigation equations require starting values for position, velocity and attitude. These are readily available from the last epoch of an ongoing iteration, but for the first epoch the INS must be specifically provided with this information before it can begin to function. This process is called initialization for position and velocity, and is called alignment for attitude (Groves Dec 2007).

### 4.15.1 Position and Velocity Initialization

Position can be initialized using a vehicle's last known position before it started to move. For a system where the INS is integrated with other systems, typically GPS, a position can easily be provided by the external navigation system. In some cases the starting point is known a priori (for example a pre-surveyed location). If the vehicle is stationary then the velocity initialization can be made with zero input. If it is moving, the initial velocity can be provided by an external navigation source such as GPS, Doppler or an odometer.

### 4.15.2 Attitude Alignment

Attitude alignment involves two steps. First, the platform is leveled by initializing the pitch ( $p$ ) and roll ( $r$ ) angles, and then gyro-compassing to provide an initial value of the heading (alternatively known as the yaw angle ‘y’ or azimuth ‘A’).

#### 4.15.2.1 Accelerometer Leveling

With the vehicle held stationary, accelerometers measure the components of the reaction to gravity due to the pitch and roll angles (i.e. the tilt with respect to the horizontal plane). The accelerometer measurements are in the body frame and can be expressed as

$$\begin{aligned}\mathbf{f}^b &= R_b^l(-\mathbf{g}^l) \\ &= (R_b^l)^T(-\mathbf{g}^l)\end{aligned}\quad (4.60)$$

where the rotation matrix  $R_b^l$  is defined as

$$R_b^l = \begin{bmatrix} \cos y \cos r - \sin y \sin p \sin r & -\sin y \cos p & \cos y \sin r + \sin y \sin p \cos r \\ \sin y \cos r + \cos y \sin p \sin r & \cos y \cos p & \sin y \sin r - \cos y \sin p \cos r \\ -\cos p \sin r & \sin p & \cos p \cos r \end{bmatrix} \quad (4.61)$$

and the gravity vector  $\mathbf{g}^l$  is defined as

$$\mathbf{g}^l = [0 \ 0 \ -g]^T$$

Substituting these values into Eq. (4.60) gives

$$\mathbf{f}^b = \left( \begin{bmatrix} \cos(y) \cos(r) - \sin(y) \sin(p) \sin(r) & -\sin(y) \cos(p) & \cos(y) \sin(r) + \sin(y) \sin(p) \cos(r) \\ \sin(y) \cos(r) + \cos(y) \sin(p) \sin(r) & \cos(y) \cos(p) & \sin(y) \sin(r) - \cos(y) \sin(p) \cos(r) \\ -\cos(p) \sin(r) & \sin(p) & \cos(p) \cos(r) \end{bmatrix} \right)^T \begin{pmatrix} 0 \\ 0 \\ -g \end{pmatrix} \quad (4.62)$$

$$\mathbf{f}^b = \begin{bmatrix} \cos(y) \cos(r) - \sin(y) \sin(p) \sin(r) & \sin(y) \cos(r) + \cos(y) \sin(p) \sin(r) & -\cos(p) \sin(r) \\ -\sin(y) \cos(p) & \cos(y) \cos(p) & \sin(p) \\ \cos(y) \sin(r) + \sin(y) \sin(p) \cos(r) & \sin(y) \sin(r) - \cos(y) \sin(p) \cos(r) & \cos(p) \cos(r) \end{bmatrix} \begin{bmatrix} 0 \\ 0 \\ g \end{bmatrix} \quad (4.63)$$

$$\begin{bmatrix} f_x \\ f_y \\ f_z \end{bmatrix} = \begin{bmatrix} -g \cos(p) \sin(r) \\ g \sin(p) \\ g \cos(p) \cos(r) \end{bmatrix} \quad (4.64)$$

From Eq. (4.64) we can calculate the pitch and roll angles as

$$p = \tan^{-1} \left( \frac{f_y}{\sqrt{f_x^2 + f_z^2}} \right) \quad (4.65)$$

$$r = \tan^{-1} \left( \frac{-f_x}{f_z} \right) \quad (4.66)$$

#### 4.15.2.2 Gyrocompassing

As well as potentially being sensitive to the Earth's rotation rate, a gyroscope will measure the rotation of the body frame with respect to the e-frame, hence

$$\omega_{ib}^b = \omega_{ie}^b + \omega_{eb}^b \quad (4.67)$$

Because the sensor triad is required to be stationary for the calibration process, the second term on the right-hand side of this equations is zero, and

$$\begin{aligned} \omega_{ib}^b &= \omega_{ie}^b + 0 \\ \omega_{ib}^b &= R_e^b \omega_{ie}^e \\ \omega_{ib}^b &= R_l^b R_e^l \omega_{ie}^e \\ \omega_{ib}^b &= (R_b^l)^T (R_l^e)^T \omega_{ie}^e \end{aligned} \quad (4.68)$$

where, the rotation matrix  $R_b^l$  is defined in Eq. (4.61) and the rotation matrix  $R_l^e$  is given as

$$R_l^e = \begin{bmatrix} -\sin \lambda & -\sin \varphi \cos \lambda & \cos \varphi \cos \lambda \\ \cos \lambda & -\sin \varphi \sin \lambda & \cos \varphi \sin \lambda \\ 0 & \cos \varphi & \sin \varphi \end{bmatrix}$$

and

$$\omega_{ie}^e = [0 \ 0 \ \omega_e]^T$$

The term  $\omega_e$  is the Earth's rotation about its spin axis, which is approximately 15.04 deg/h.

By substituting the expressions for  $R_b^l$ ,  $R_l^e$  and  $\omega_{ie}^e$  into Eq. (4.68), we get

$$\begin{aligned} \omega_{ib}^b &= \begin{bmatrix} \cos(y) \cos(r) - \sin(y) \sin(p) \sin(r) & \sin(y) \cos(r) + \cos(y) \sin(p) \sin(r) & -\cos(p) \sin(r) \\ -\sin(y) \cos(p) & \cos(y) \cos(p) & \sin(p) \\ \cos(y) \sin(r) + \sin(y) \sin(p) \cos(r) & \sin(y) \sin(r) - \cos(y) \sin(p) \cos(r) & \cos(p) \cos(r) \end{bmatrix} \\ &\quad \begin{bmatrix} -\sin \lambda & \cos \lambda & 0 \\ -\sin \varphi \cos \lambda & -\sin \varphi \sin \lambda & \cos \varphi \\ \cos \varphi \cos \lambda & \cos \varphi \sin \lambda & \sin \varphi \end{bmatrix} \begin{bmatrix} 0 \\ 0 \\ \omega_e \end{bmatrix} \end{aligned} \quad (4.69)$$

$$\omega_{ib}^b = \begin{bmatrix} \cos(y) \cos(r) - \sin(y) \sin(p) \sin(r) & \sin(y) \cos(r) + \cos(y) \sin(p) \sin(r) & -\cos(p) \sin(r) \\ -\sin(y) \cos(p) & \cos(y) \cos(p) & \sin(p) \\ \cos(y) \sin(r) + \sin(y) \sin(p) \cos(r) & \sin(y) \sin(r) - \cos(y) \sin(p) \cos(r) & \cos(p) \cos(r) \\ 0 \\ \omega_e \cos \varphi \\ \omega_e \sin \varphi \end{bmatrix} \quad (4.70)$$

$$\begin{bmatrix} \omega_x \\ \omega_y \\ \omega_z \end{bmatrix} = \begin{bmatrix} \{\sin(y) \cos(r) + \cos(y) \sin(p) \sin(r)\} \omega_e \cos \varphi - \omega_e \cos(p) \sin(r) \sin \varphi \\ \omega_e \cos \varphi \cos(y) \cos(p) + \omega_e \sin \varphi \sin(p) \\ \{\sin(y) \sin(r) - \cos(y) \sin(p) \cos(r)\} \omega_e \cos \varphi + \omega_e \sin \varphi \cos p \cos(r) \end{bmatrix} \quad (4.71)$$

Since the pitch angle  $p$  and roll angle  $r$  were already obtained during the accelerometer leveling process using Eqs. (4.65) and (4.66) respectively, we will now use the three gyro measurements to obtain the yaw angle  $y$ . It is evident from Eq. (4.71) that if the gyro measurement  $\omega_x$  is multiplied by  $\cos(r)$  and the gyro measurement  $\omega_z$  is multiplied by  $\sin(r)$  then

$$\omega_x(\cos r) + \omega_z(\sin r) = (\omega_e \cos \varphi) \sin y \quad (4.72)$$

Similarly

$$\omega_y(\cos p) + \omega_x(\sin p \sin r) - \omega_z(\cos r \sin p) = (\omega_e \cos \varphi) \cos y \quad (4.73)$$

Consequently

$$\tan y = \frac{\omega_x(\cos r) + \omega_z(\sin r)}{\omega_y(\cos p) + \omega_x(\sin p \sin r) - \omega_z(\cos r \sin p)} \quad (4.74)$$

Finally the yaw angle is

$$y = \tan^{-1} \left[ \frac{\omega_x(\cos r) + \omega_z(\sin r)}{\omega_y(\cos p) + \omega_x(\sin p \sin r) - \omega_z(\cos r \sin p)} \right] \quad (4.75)$$

For land vehicle applications, where the vehicle travels is almost a horizontal plane, the pitch and roll angles are close to zero and the small angle approximation yields

$$\begin{aligned} \cos r &= \cos p \approx 1 \\ \sin r &= \sin p \approx 0 \end{aligned} \quad (4.76)$$

Equation (4.75) now reduces to

$$y = \tan^{-1} \left( \frac{\omega_x}{\omega_y} \right) \quad (4.77)$$

It should be noted that gyro-compassing is not feasible for low grade IMUs, which cannot detect the Earth's rotation because their noise threshold exceeds the signal for the Earth's rotation. For these IMUs a heading (yaw angle) is obtained externally using either a compass or a magnetometer. For systems integrated with

GPS, the east and north velocities supplied by this system provide a heading after the host platform has started to move. In this case the heading is

$$y = -\tan^{-1}\left(\frac{v_e}{v_n}\right) \quad (4.78)$$

where  $v_e$  is east velocity and  $v_n$  is north velocity.

## References

- Barbour N, Schmidt G (2001) Inertial sensor technology trends. *Sens J IEEE* 1(4):332–339
- Grewal MS, Weill LR, Andrews AP (2007) Global positioning systems, inertial navigation, and integration, 2nd edn. Wiley, New York
- Groves PD (2007) Principles of GNSS inertial and multi-sensor integrated navigation systems. Artech House, USA
- KVH (2012) [www.kvh.com/Commercial-and-OEM/Gyros-and-Inertial-Systems-and-Compasses/Gyros-and-IMUs-and-INS.aspx](http://www.kvh.com/Commercial-and-OEM/Gyros-and-Inertial-Systems-and-Compasses/Gyros-and-IMUs-and-INS.aspx). Accessed 28 Mar 2012
- Lawrence A (1998) Modern inertial technology: navigation, guidance, and control, 2nd edn. Springer, New York
- Petovello M, Lachapelle G, Scherzinger B (2007) What are the important considerations when selecting the type of quality of IMU for integration with GNSS. InsideGNSS
- Prasad R, Ruggieri M (2005) Applied satellite navigation using GPS GALILEO and augmentation systems. Artech House, USA
- Wang, HG, Williams TC (2008) Strategic inertial navigation systems-high-accuracy inertially stabilized platforms for hostile environments. *IEEE Control system Magazine* 28(1):65–85